IRAM Newsletter

Number 54 December 20th , 2002

Contents

Calendar

March 3rd, 2003 17:00h (MET):
Deadline for the submission of observing proposals for the period May 15, 2003 to Nov 15, 2003

April 3/4, 2003
IRAM Program Committee meeting (provisional date)

Personnel Changes

IRAM GRENOBLE

Since September 23rd, Fanny CORSET is working in the scientific software group in Grenoble. The receiver group welcomes Patrice SERRES (who did arrive on September 30th), David BOUTEBBA (October 7th) and Rachid SMAOUI (November 4th).

On December 1st, Robert ZYLKA has joined the Grenoble astronomer's group after two years at the Ersten Physikalischen Institut der Universität zu Köln, Germany. Besides his astronomical activities, he will continue his work on bolometer data reduction software.

Michael BREMER

IRAM Program Committee Recommendations

The IRAM program committee convened in Grenoble on October 17 and 18 to discuss the proposals submitted for the winter 2002/2003 scheduling period. The committee

PdBI Proposal Ratings

Project	Rate	Project	Rate	Project	Rate
M022	A[1]	M023	C	M024	C
M025	B	M026	B	M027	A
M028	A[2]	M029	B[2]	M02A	B
M02B	B	M02C	B	M02D	B
M02E	B	M02F	C	M030	A[3]
M031	A	M032	A	M033	B
M034	A	M035	B[2]	M036	B[2]
M037	C	M038	A	M039	A
M03A	C	M03B	C	M03C	C
M03D	C	M03E	B	M03F	B[2]
M040	A[1]	M041	B[2]	M042	A
M043	B	M044	A	M045	C
M046	A	M047	A	M048	C
M049	B	M04A	C	M04B	B
M04C	B	M04D	B	M04E	B
M04F	B	M050	B[2]	M051	B[2]
M052	C	M053	C	M054	B
M055	A	M056	A	M057	B
M058	B[2]	M059	C	M05A	C
M05B	B[2]	M05C	B	M05D	A
M05E	B[2]	M05F	A	M060	A
M061	A	M062	B	M063	B
M064	A	M065	B	M066	B[2]
M067	B	M068	B	M069	B
M06A	B[2]	M06B	B[2]	M06C	B
M06D	C				

[1] program rated B and C in one or more parts

[2] program rated B in one or more parts

[3] program rated C in one or more parts

30-M Proposal Ratings

A	B		C
086-02	087-02	135-02	093-02
088-02∗	088-02∗	136-02	094-02
095-02	089-02	138-02	097-02
102-02	090-02	139-02	099-02
103-02	091-02	140-02	104-02
107-02	092-02	141-02	105-02
109-02	096-02	145-02	108-02
114-02	098-02	147-02	112-02
118-02∗	100-02	153-02	113-02
121-02	101-02	158-02	144-02
126-02	106-02	162-02	146-02
131-02	110-02	163-02	150-02
134-02	111-02	165-02	152-02
137-02	115-02	166-02	154-02
142-02	116-02	167-02	155-02
143-02	117-02	170-02	156-02
148-02	118-02∗	173-02	157-02
149-02	119-02	174-02	169-02
151-02	120-02	175-02	171-02
159-02	122-02	178-02	176-02
160-02	123-02	180-02	177-02
161-02	124-02	181-02	179-02
164-02	125-02	182-02	184-02
168-02	127-02	183-02	189-02
172-02	128-02	185-02	
188-02	129-02	186-02	
	130-02	187-02	
	132-02	190-02	
	133-02		

∗ part of proposal

was chaired by Linda Tacconi (MPE, Munich). The principal investigators of each proposal will also be informed by letter which will include comments issued by the committee if there are any.

PLATEAU DE BURE INTERFEROMETER PROPOSALS

A total of 76 proposals were received for the interferometer. The programs were classified A (accepted), B (backup) and C (rejected). Programs rated A will be scheduled in priority. Further time, if it becomes available, will go to the B programs, taking into account scientific merit, crowding in certain right ascension ranges and general aspects of balance.

For projects rated A and B and without IRAM internal collaborator, please consult the list of local contacts on the IRAM web pages `http://www.iram.fr/GENERAL/loc_sep02.txt`.

30M PROPOSALS

105 proposals were received for the 30m telescope, requesting 4426.5 hours of telescope time. The highest rating “A” was given to 26 proposals; 55 proposals were rated “B”, i.e. were given backup status. The remaining proposals, although scientifically valuable in most cases, were rated “C”. The individual ratings are listed in the attached table. All A-rated proposals will be scheduled on the telescope, although some with less time than requested. We expect that about half of the B-rated programs will actually be scheduled. The selection will take into account scientific merit, crowding in certain right ascension ranges, and general aspects of balance. Proposals rated ”C” will not get telescope time.

Roberto NERI and Clemens THUM

Plateau de Bure as a VLBI phased array station

After the successful VLBI experiment in 1995 at 86 GHz and 215 GHz between one antenna of the IRAM Plateau de Bure interferometer (PdB, France) and the IRAM 30–m telescope (PV, Spain) (Greve et al. 1995, Krichbaum et al. 1997), the decision was taken to equip PdB as

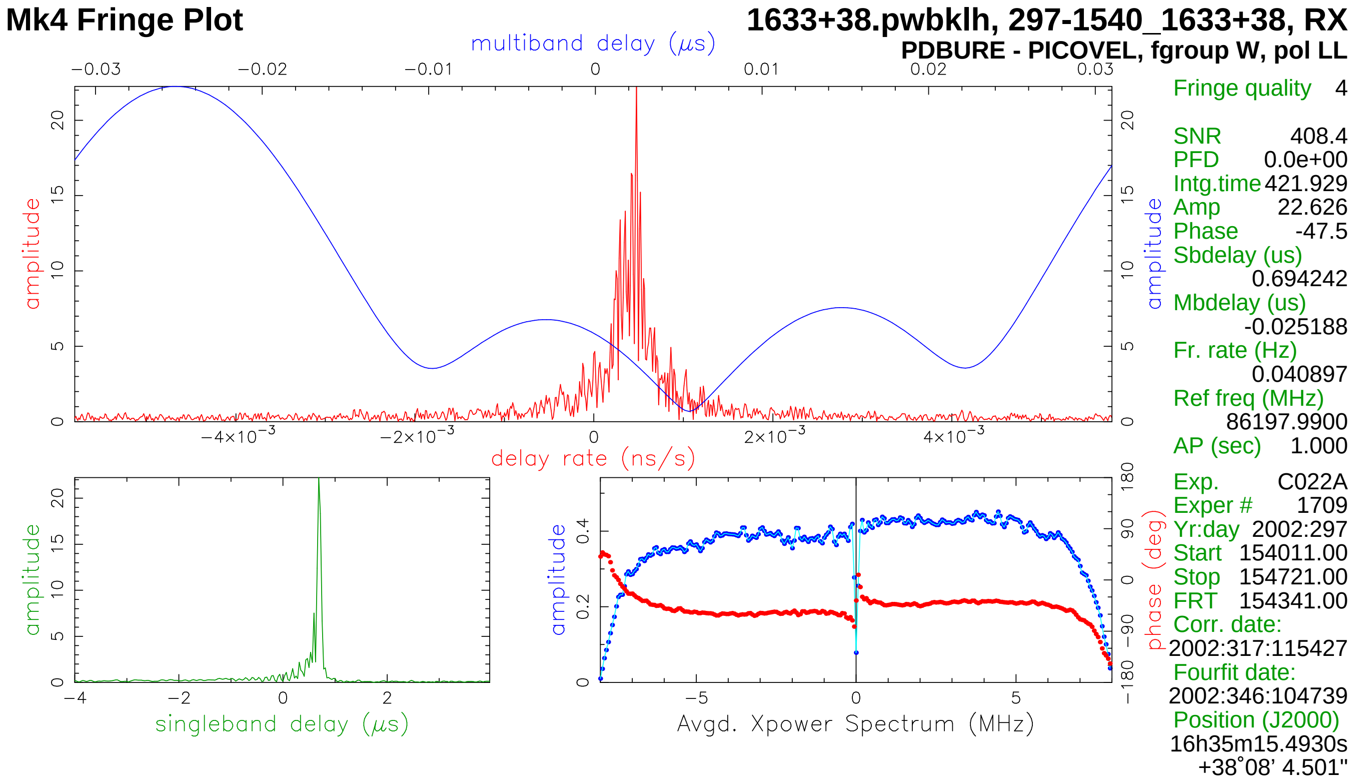

Figure 1: MK4 Fringe plot on the quasar 1633+38 at 86.198 GHz between the Plateau de Bure and Pico Veleta, observed on October 24th during the global VLBI session. The S/N ratio is higher than 400.

a permament station for global VLBI observations, using the six 15–m diameter antennas as a combined phased array at 3 mm (100 GHz) or 1.3 mm (230 GHz) wavelength. In July 2002 it became possible to bring by helicopter the necessary equipment for VLBI observations to Bure i.e. the maser, the tape recorder, the formatter and decoder, and the VLBI FS9 control computer.

Tests took place on October 8th and 9th,2002 at 86 – 89 GHz (3.5 mm) on the 685 km long baseline between the 6–element phased array of the PdB Interferometer (France) and the 100–m telescope at Effelsberg telescope (EFF; MPIfR, Germany). The length of the baseline between PdB and EFF is 685 km, in the direction North–South. Unfortunately, the IRAM 30–m telescope was not available because of continuously poor weather conditions. Even so, a S/N ratio of several hundred with an angular resolution of about 0.9 milli-arcsec was achieved.

Thereafter the 6–element Plateau de Bure phased array participated in late October 2002 in the last CMVA coordinated global 3 mm VLBI observing campaign. The IRAM 30–m did also participate, this time under excellent weather conditions. A first fringe plot between the two IRAM instruments is shown in Fig. 1. The intention is to use PdB from now on as a regular VLBI telescope.

The VLBI team:
D.A. Graham, M. Torres, D. Broguiere, R. Lucas, T.P. Krichbaum, M. Bremer, A. Grosz, B. Rossini, M. Grewing, S. Sanchez, IRAM and MPIFR logistics staff, the Bure, Effelsberg and Pico Veleta telescope Operators, the MPIfR correlator team, J.M. Torre (CERGA, H-maser),
organized by A. Greve

BIBLIOGRAPHY

– Greve A., Torres M., Wink J.E. et al. 1995, A&A 299, L 33

– Krichbaum T.P., Graham D.A., Greve A. et al. 1997, A&A 323, L 17

New IRAM web site

On December 16th, the official switch took place from the old IRAM web site on `http://iram.fr` to the new site on `http://www.iram.fr`. The advantage of the new pages is the daily mirroring between IRAM Granada and IRAM Grenoble, which allows users to switch between `http://www.iram.es` and `http://www.iram.fr` according to their location and/or web traffic.

The new web site has already out-grown the old one. Some important information pages will be maintained for a transitional period on both sites, but bookmarked pages should soon be updated.

As always, problems may arise from the use of different web browsers (versions and operating systems) which may not be noticed immediately during the development. If you encounter a problem, don't hesitate to send a mail to the webmaster (bremer@iram.fr).

Many thanks to the past and present members of the IRAM web group who have developed the pages: Virginie Guérard, Catherine Berjaud, Fabienne Rossini, Rosa Montalban, Rainer Mauersberger, Roberto Neri, Marc Torres, and many others. Of course, such a site could not function without the support of the system managers Alain Perrigouard (Grenoble) and Walter Brunswig (Granada).

More pages are planned: general information in several languages, a dedicated VLBI section, and of course press releases of the latest observing results whenever the PIs agree.

Michael BREMER

News from the 30m Telescope

IRAM DATABASE FOR POOLED OBSERVATIONS

All informations on projects taking part in the pooled observing mode are now stored in our new database system. The database has a web interface which allows to access and modify all information relevant to pooled observing via a web browser.

Projects taking part in the pooled observing mode will have a project account from which PIs can store in the database all instructions necessary to carry out the observations. In turn this account allows the PIs to monitor the progress of their project: each scan taken for a project is displayed together with some basic information such as the date, observing mode and scan duration. Additional comments visible to the PI may be inserted by the observers at the telescope.

To allow a quick look at the data we provide a pipeline NIC reduction for bolometer observations. It allows the user to reduce maps and on/off observations online without downloading the data.

For further data analysis the PIs can download their data via their web browser. Together with the data files, the PIs will retrieve the observing log(s), all macros and catalog files related to the observations and a summary on all scans taken for the project.

Based on the progress in of his project a PI can change the priority of his sources, modify the observing instructions or make comments for observations on individual sources.

All information entered by the PIs is directly accessible to the observers at the telescope. Besides the detailed observing instructions the database provides additional tools for carrying out the observations. Among those are astronomical tools to provide information on visibility of sources and fluxes for all calibrators, as well as project source listings which take into account project priorities and the current weather conditions.

The final decision which sources to observe is made by the pool coordinator at the telescope taking into account visibility, priority and the observing conditions.

A more detailed description of the database will soon be available on our web pages. For more information about the pooled sessions and the database contact `aweiss@iram.es`.

Axel WEISS

MOBILE PHONE INTERFERENCES IN THE FILTER BANK BACKEND

This article demonstrates the disturbance effect that the GSM service for mobile phones produces in the 30-m filter bank backend.

The GSM service uses the frequency bands 890-915 MHz for the uplink (mobile station to base station) and 935-960 MHz for the downlink (base station to mobile station). An interference in the backend spectrum should be produced by the mobile station when transmitting close to the backend electronics.

The following measurements have been done using the 1 MHz filter bank in the broad band configuration, which means 1024 channels of 1 MHz covering the IF range from 86 to 1110 MHz.

Previously, a calibration (CAL COLD procedure) was done with the A230 receiver tuned at 230 GHz. Then the IF cable was disconnected from the receiver and connected to a 50 Ω load in order to remove the receiver noise from the spectrum. Under these conditions several spectra were taken with a mobile phone transmitting from different distances. Each spectrum consists of two subscans of 3 minutes integration time each. With repetitive conditions results are similar. A summary of all the spectra taken is shown in the following graphics.

In Fig. 2a) shows a reference spectrum when no transmission from a mobile phone is present. Both subscans are similar and the superimposed noise is something intrinsic to the backend and the acquiring data procedure.

In Fig. 2b) a spectrum was taken while a mobile phone was continuously transmitting during the 3 minutes of the first subscan, at a distance of 2 meters of the filter

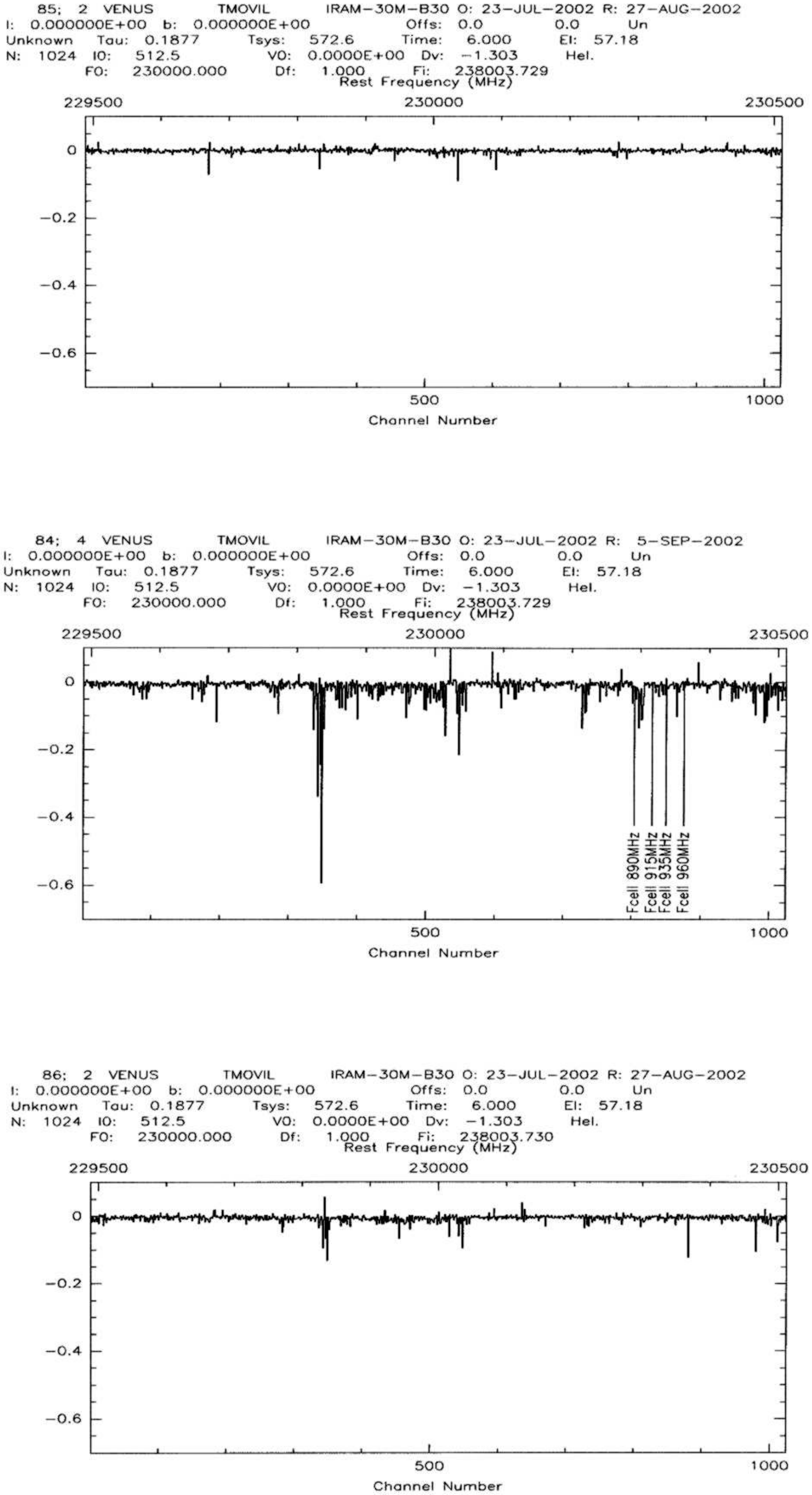

Figure 2: **a)** (top) no mobile phone transmission, **b)** (middle) mobile phone transmission at 2 meters distance, **c)** (bottom) mobile phone transmission at 8 meters distance.

bank electronics inside the backend/computer room. During the second subscan the mobile phone was switched off. Frequencies of the GSM band pass range are indicated, but the corruption extends over the whole 1 GHz band pass frequency.

Figure 2c) finally shows a spectrum taken under similar conditions as the previous one, but with the mobile phone transmitting from the corridor between the backend-computer room and the library, at a distance of approx. 8 meters to the filter bank electronics.

Assuming that

- a typical mobile phone conversation lasts 3 minutes,
- the disturbance noise in the spectra has a noise level of 100 mK at a distance of 8 meters,
- the mobile phone disturbance effect decreases with the square of the distance,
- a reasonable observing threshold is below 1 mK,

we conclude that a mobile phone should never transmit at a distance shorter than 70 meters to the filter bank electronics when the telescope is operating.

Juan PEÑALVER and Salvador SANCHEZ

VESPA is operational

The thorough upgrade of the 4096 channel autocorrelator at the 30m telescope is now complete. The new correlator backend named VESPA (**VE**rsatile **SP**ectrometer **A**ssembly) combines hardware from the old 30m and interferometer correlators in a powerful new design. The control and data acquisition software is working, and VESPA is available for general use since May giving the 30m a much needed boost in acquisition power for high resolution data. The hardware is organized in 6 units (Fig. 3). Each digital chassis contains 12 correlation boards of 256 delay channels.

A total of 18 432 time domain channels are now available. With two synthesizers installed in each unit, a large range of spectral resolutions and bandwidths become possible, increasing the correlator capabilities by a factor 3 in most configurations. In addition, new user modes, not available in the old 30m correlator, have been installed, increasing performance further. Table 1 summarises the capabilities of VESPA in its 4 user modes.

A full representation of its complexity is not possible here. Interested readers are referred to the VESPA users guide[1] and to a more technical summary at `http://www.iram.fr/IRAMFR/TA/backend/`. A very detailed graphical configurator program (written in python) can be downloaded from `http://www.iram.fr/IRAMFR/PV/vespaconf.py`.

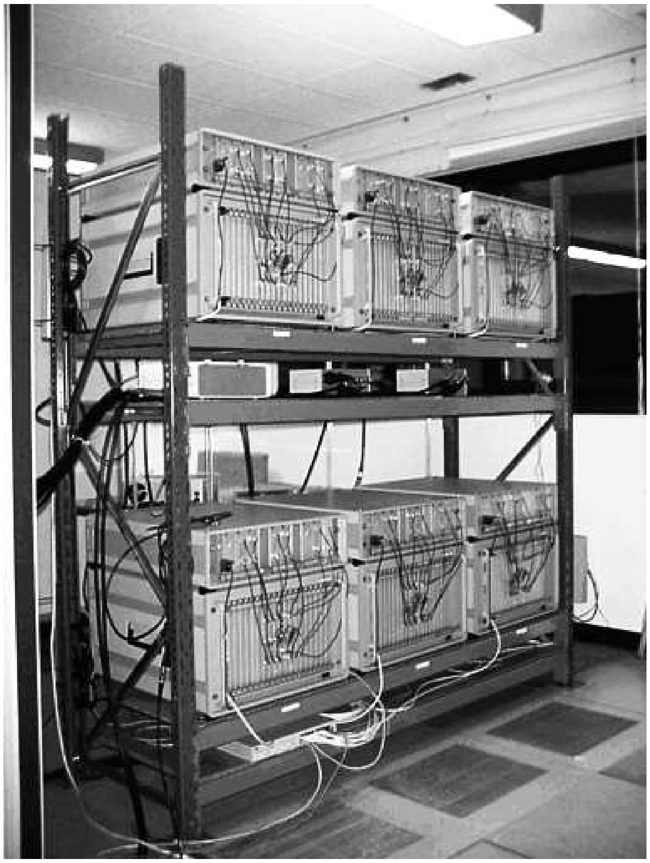

Figure 3: VESPA in the backend room at the 30m telescope. This correlation spectrometer consists of 6 units, each having a digital chassis with 12 correlator boards and an analog chassis with 15 RF modules.

VESPA is used in its **basic mode** to connect to the (single pixel) SIS receivers. This is the most flexible mode, since any user defined spectral band can be connected to any of the 4 receivers in a valid configuration. Each spectral band can be individually moved to any IF frequency in the range 100 to 600 MHz. Table 1 shows that up to 12 spectral bands are available for the common spectral resolutions ($\geq$ 20 kHz). In particular, individual bands can be joined to form one contiguous spectral band connected to one receiver. A maximum bandwidth of 480 MHz can thus be covered at the often useful spectral resolution of 40 kHz.

VESPA extends this basic mode towards spectral resolutions of 10 kHz and smaller. In these **extra high resolution modes** an unprecedented velocity resolution of 10 m/s is reached at 100 GHz. Observations of the coldest molecular clouds profit from this high spectral resolution (Fig. 4) and small differential motions between parts of such clouds can now be studied. The corresponding requirement on the frequency stability due to the various Doppler corrections is, however, challenging and needs more study.

In sensitivity–limited observations it is advantageous

---

[1] `http://www.iram.es/IRAMES/otherDocuments/manuals/vespa_ug.ps`

Table 1: VESPA user modes. Bandwidths are nominal values, the spectral resolution column lists channel separation.

	basic	**parallel**		**multi—beam**	**polarimetric**	
resolution kHz	sections $\times$ bandwidth $N\times$ MHz	receiver pairs one	two	sections $\times$ bandwidth $N\times$ MHz	receiver pairs one	two
3.3	6×10 — 1×60					
6.6	6×20 — 1×120					
10	6×20 — 1×120					
20	12×20 — 1×240	180	60, 120	2×20 — 1×40		
40	12×40 — 1×480	360	120, 240	4×20 — 1×80	120	40, 80
80	12×40 — 1×480	480	160, 320	4×40 — 1×160	240	80, 160
320	12×80 — 1×640	640	320, 640	4×80 — 1×320		
625					480	160, 320
1250	12×160 — 1×640	640	640, 640	4×160 — 1×640		
2500					640	240, 480

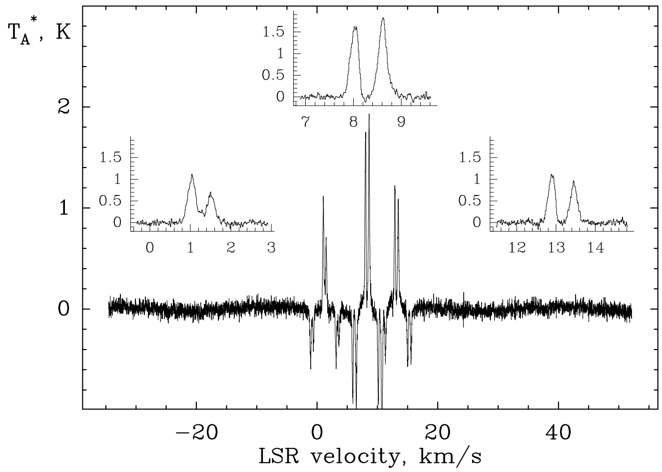

Figure 4: HCN Spectrum (88 GHz) of a cold dark cloud showing the combined effects of hyperfine splitting, optical depth, and velocity structure. The spectrum was obtained with VESPA at a resolution of 3.3 kHz (11 m/s) and 30 MHz bandwidth in frequency switching mode. The insets display the 3 velocity–resolved hyperfine components.

to use two (orthogonally polarized) receivers tuned to the same frequency. The **parallel mode** of VESPA supports this frequent observing strategy. Inasmuch as possible, VESPA employs a single synthesizer for parallel bands, leaving the other synthesizer for additional bands or a larger contiguous band. Table 1 shows the maximum contiguous band available at a given resolution for each receiver in such a pair of parallel receivers. VESPA can also be configured (not shown in the Table) in several narrower parallel bands whose combined width does not exceed the maximum listed in the table. Even two pairs of parallel receivers can be handled in this mode. The table gives maximum bandwidths for each pair.

The main use of VESPA will probably be with the multi–beam 1.3mm SIS receiver HERA which has currently a center–filled square array of 9 beams. In its **multi–beam mode** VESPA constitutes an efficient spectrometer offering resolutions from 20 kHz to 1.25 MHz with bandwidths shown in the table. At the frequently used resolution of 80 kHz, VESPA provides one band of 160 MHz or 2(4) independent bands of 80(40) MHz for *each* of the 9 beams. These bandwidths per beam will be halved however, when HERA is upgraded to 18 beams.

Fortunately, during the assembly of VESPA, not all the memory of the origin of most of its hardware was erased. VESPA has retained the capability of doing cross correlations which was its main function at the IRAM interferometer. In its **polarimetric mode**, VESPA cross correlates the IF powers from two orthogonally polarized receivers tuned to the same frequency. Stokes U and V spectra can thus be derived when linearly polarized receivers are used. Apart from the superiority of fully digital correlations over analog correlations, VESPA polarimetry also offers much more bandwidth than the 40 MHz available with the IF polarimeter (see Tab. 1). Several questions of calibration have still to be studied, however, before the polarimetric mode can be made available.

VESPA was designed by G. Paubert in collaboration with the Grenoble backend group headed by M. Torres. Ph. Chavatte, A. Lapinov, J.Y. Mayvial, Th. Merrien, and A. Sievers, and M. Vidal were actively contributing at various stages of this 1.5 year project.

G. Paubert & C. Thum

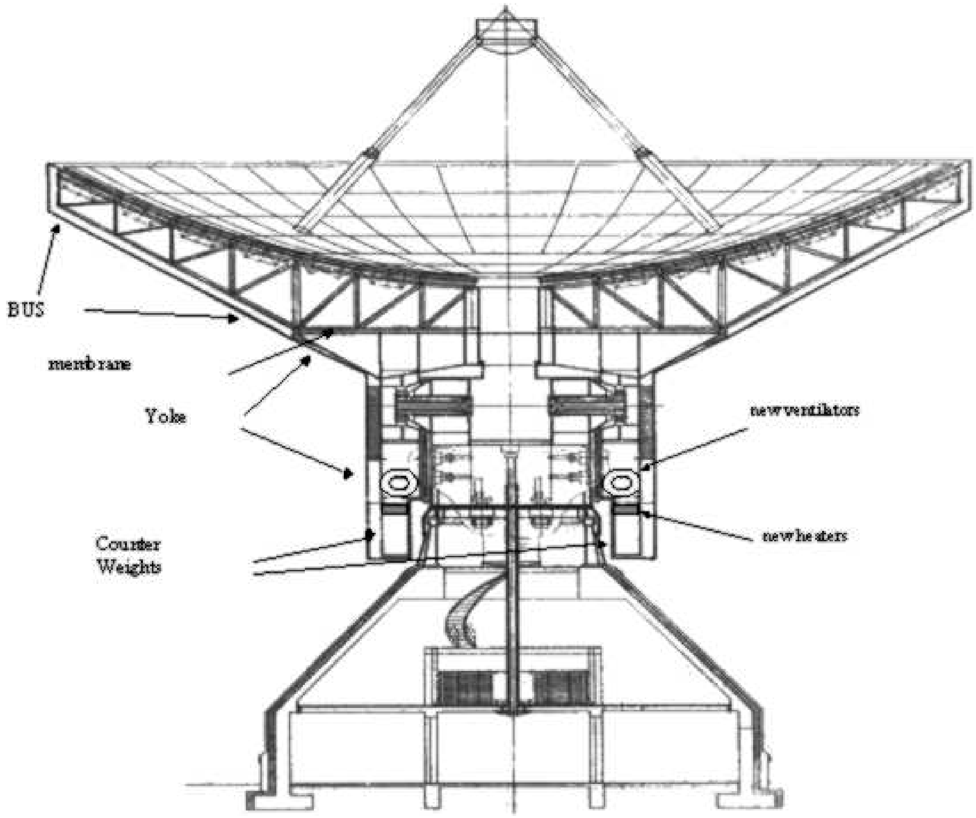

Figure 5: The 30-m telescope and the position of the new Temperature Control System

First results of the IRAM 30-m telescope improved thermal control system

The structure of the 30–m telescope is made of steel and the design aimed from the beginning at the minimisation of its thermal deformations. For this purpose the antenna steel structure is covered with thermal insulation. In addition, the Reflector Backup Structure (BUS) is equipped with an active cooling/heating thermal control system (TCS) maintaining the temperature homogeneity of the BUS within 1 K.

Figure 5 shows a cross–section through the 30–m telescope. The strict conical design of the BUS is terminated in a flat circular steel surface, called the membrane. Below the membrane are the Yoke and both Counter Weight arms, one at each lateral side of the antenna.

The initial TCS controls only the temperature of the BUS. Five ventilators apply a tangential air circulation with a heating/cooling capacity of 30/22 kW. A temperature sensor installed in the upper part of the Yoke, below the membrane, measures the reference temperature to which the temperature of the BUS and the feed legs is slaved. The initial TCS does not apply temperature control to the Yoke and the Counter Weights.

During the past years, 174 temperature sensors were installed in the BUS, Yoke and Counter Weights and also in the TCS fluids of the feed legs in order to monitor the temperature of the whole antenna. In a further step, a Finite Element Model (FEM) was developed to interpret the measured antenna temperatures with respect to the antenna performance. The predictions of the FEM have been confirmed from dedicated focus and holography measurements. The FEM permits a decomposition of the calculated temperature–induced reflector surface deformations into large–scale contributions represented in Zernike polynomials; from these we found that the dominant components of reflector surface deformations are astigmatism (of amplitude α_2), and 3rd order defocus (of amplitude α_4). It was recommended to improve the thermal homogeneity of the upper part of the Yoke, just below the membrane.

An independent forced ventilation system, consisting of 4 ventilators moving the air in a circular way, was installed in the upper part of the Yoke in autumn 1999. The temperature of this part of the telescope structure was improved. Nevertheless, the reflector astigmatism still showed a permanent high value though with less variation than previously observed, which was due to temperature inhomogeneities of the yoke.

A sample of the performance of the initial TCS, with the ventilators at the upper Yoke working, for a period of 5 days with good weather, clear sky, low wind and

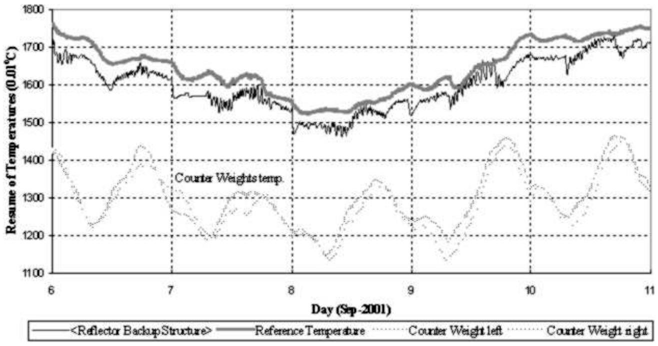

Figure 6: Initial Temperature Control System during five days of good weather: Temperatures of the BUS and counterweights.

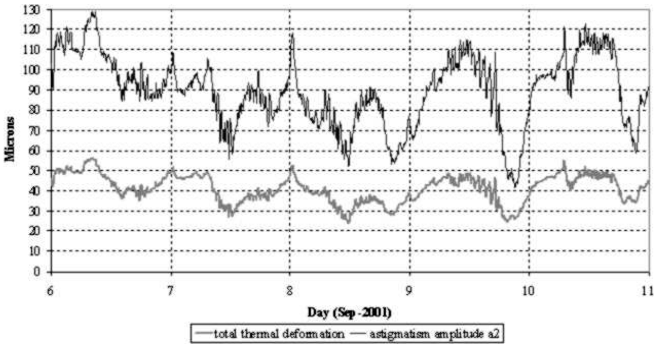

Figure 7: Initial Temperature Control System during five days of good weather: Temperature induced rms thermal deformations and amplitude α_2 of the astigmatism.

the antenna observing all the time is shown in Figs. 6 and 7. After analysing the information from the temperature sensors and the FEM we concluded the following:

a) the initial TCS works well and the controlled temperature of the BUS is homogeneous within 1 K (Figure 6). This behaviour fulfils the design specifications.
b) the Counter Weights are always approximately 3 K cooler than the reference temperature (Figure 6). The reason for this difference is the extra heating applied to the BUS and the upper Yoke, which comes mainly from the ventilators inside the BUS, the cooling compressor of the TCS, and the conducted heat from the receiver room inside the antenna structure. The Counter Weights are less strongly coupled to the internal heating sources and more to the open air. In general, the reference for regulation of the BUS is 4 to 7 K above the average temperature.
c) Figure 7 shows the prediction from the FEM of the total thermal rms deformations of the reflector surface σ_{T} and the amplitude α_2 of the temperature–induced astigmatism, derived from the decomposition into Zernike polynomials. The displayed amplitudes α_2 are between 40–120 μm.

When using the FEM to analyse the reflector astigmatism versus the antenna temperature distribution for a long period of time we noticed that occasionally the amplitude of the astigmatism is small. This situation occurs when the air temperature drops rapidly due to some particular meteorological condition. The BUS and Yoke temperatures decrease faster than the temperature of the Counter Weights due to their lower inertia, and at a certain moment the temperatures of these three components are equal. At this moment the astigmatism disappears.

According to the FEM a certain temperature gradient in the Counter Weights has a smaller effect than a similar gradient in the Yoke. On the other hand, the temperature difference between the Counter Weights and the reference temperature is much higher than the temperature difference between the Yoke and the reference temperature. We decided to modify the TCS by applying heat to the Counter Weights in order to reproduce the noticed condition of small astigmatism, i.e. of equal temperatures in the BUS, Yoke and Counter Weights.

In September of this year (during the yearly maintenance) we have made the following changes in the antenna TCS (Figure 5):

1) Two ventilators, one at each lateral side of the Yoke, were installed between the elevation axis and the Counter Weights. Each ventilator moves 4 300 m^3/h of air around the elevation axis at the corresponding lateral side of the Yoke, equalising the temperature between the Counter Weights and the upper part of the Yoke. Both ventilators are permanently ON.
2) Four sets of heaters, with 3 kW each, were installed in the Counter Weights, two sets per antenna lateral

Parameter		Initial TCS	New TCS
Reference – Counter Weight Temperature	[K]	3.34 (0.57)	0.26 (0.14)
Total Reflector Surface Deformation (rms–value σ_T)	[μm]	41.1 (6.9)	16.5 (4.2)
Component of Random Thermal Deformations (rms–value σ_{rd})	[μm]	16.0 (4.4)	12.5 (3.7)
Amplitude Astigmatism α_2	[μm]	89.6 (17.7)	14.5 (8.5)
Amplitude 3rd Order Defocus α_4	[μm]	18.9 (13.9)	13.3 (10.6)

Table 2: Comparison of the initial and new temperature control system

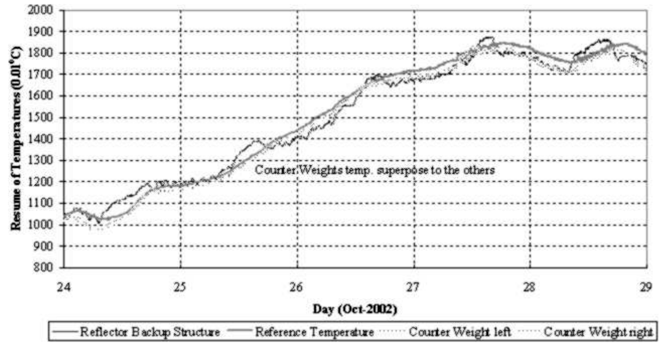

Figure 8: New Temperature Control System during five days of good weather: Temperatures of the BUS and Counterweights.

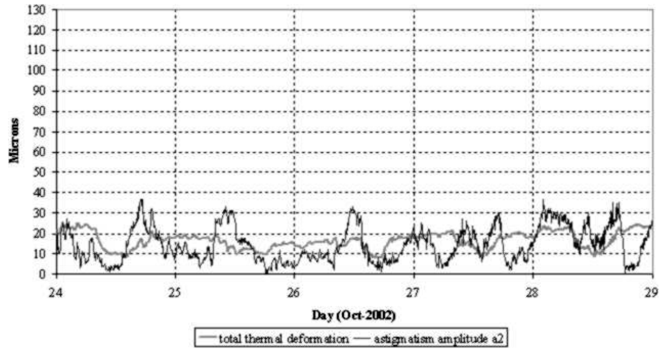

Figure 9: New Temperature Control System during five days of good weather: same as Fig. 7

side. Each heater is installed in a closed compartment to optimise the heat transfer to the Counter Weights and from there, by conduction rather than convection, to the rest of the Yoke. The number of activated heaters depends on how cold the Counter Weights are with respect to the reference temperature.

The new TCS operates since 17 October 2002. We have analysed the data of 5 days with clear sky, low wind, and with the antenna observing all the time (last VLBI session) to understand its behaviour. Results are shown in Figures 8 and 9 which illustrate the improvement reached with the new TCS. Besides the 5 days analysed so far, the new TCS is working well since its beginning of operation.

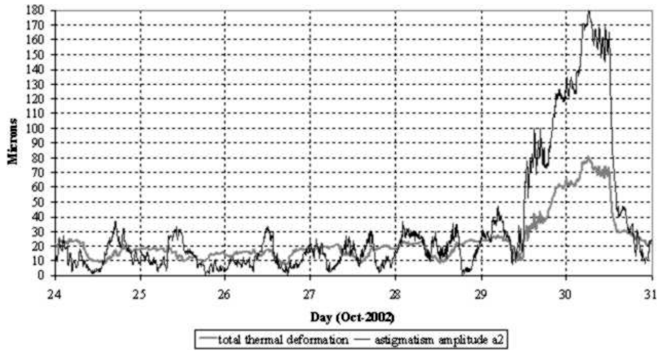

Figure 10: New Temperature Control System during five days of good weather: up to day 29 with the operation of the new TCS, from day 29 on operation of the initial TCS.

Table 2 compares the behaviour of the initial TCS and the new TCS, including the reflector performance predicted from the FEM. The values give the average and the standard deviation (rms–value).

Note that α_2 and α_4 is the amplitude of astigmatism and 3rd order defocus, respectively. The corresponding quasi rms–values of these systematic surface deformations are $\sigma_2 \approx 1/3 \times \alpha_2$ and $\sigma_4 \approx 1/3 \times \alpha_4$.

Figure 10 is similar to Figure 9 but including two more days. Between day 29.5 – 30.5 the new TCS was intentionally switched back to the initial TCS to facilitate the comparison of the performances.

With the operation of the new TCS the thermal behaviour of the antenna has improved. Several more months of data must confirm the preliminary results. However there is no reason to expect a degradation of the new TCS after working well under different meteorological conditions during 4 weeks. The goal to keep the antenna from the Reflector Backup Structure to the Counter Weight on the same temperature has been reached and so far the antenna shows a more stable thermal behaviour. Under this improved condition a new efficiency measurement as well as holography should be considered in the near future.

Juan Peñalver, Albert Greve and Michael Bremer

Scientific Results in Press

DESIGN AND CHARACTERIZATION OF 225-370 GHZ DSB AND 247-360 GHZ SSB FULL HEIGHT WAVEGUIDE SIS MIXERS

B. Lazareff(1), D. Billon-Pierron(1), A. Navarrini(1) and I. Peron(1)
(1)Institut de Radio Astronomie Millimétrique, 300 rue de la Piscine, 38406 St. Martin d'Hères, France

Abstract:

We report on the design and characterization of two full height waveguide SIS mixers for astronomical applications: a Double Side Band (DSB) fixed-tuned mixer covering the 225-370 GHz band (≈ 50 % of relative bandwidth), and a tunable Single Side Band (SSB) mixer covering the 247-360 GHz frequency range. The DSB receiver noise temperature we have measured is below 50 K over a bandwidth larger than 100 GHz for the DSB mixer and has a minimum of 27 K (uncorrected) at 336 GHz; to our knowledge this is the lowest noise ever reported at this frequency. A receiver noise temperature below 80 K and an image band rejection around -14 dB were measured over most of the band of the SSB mixer.

Both mixers use similar chips that integrate a parallel tuning inductor with a radial microstrip stub to compensate for the junction capacitance of 75 fF (junction size 1 μm^2). A stability criterion for intrinsically DSB and SSB mixers under typical operating conditions has been derived. The receiver designs have been optimised in order to guarantee a low mixer noise temperature while maintaining adequate gain and stable operation over the whole frequency bands of interest.

Apperared in: Proceedings of the 5th. European Workshop on Low Temperature Electronics (WOLTE 5), J. Phys. IV France 12 (2002), Pr3-161

WIDESPREAD HCO EMISSION IN THE NUCLEAR STARBURST OF M82

S.García-Burillo(1), J.Martín-Pintado(1), A.Fuente(1), A.Usero(1) and R.Neri(2)
(1)Observatorio Astronómico Nacional, Campus Universitario, Apartado 1143, Alcalá de Henares, E-28800 Madrid, Spain, (2)Institut de Radioastronomie Millimétrique, 300 Rue de la Piscine, F-38406 Saint Martin d'Hères, France

Abstract:

We present a high-resolution ($\sim 5''$) image of the nucleus of M82 showing the presence of widespread emission of the formyl radical (HCO). The HCO map, the first obtained in an external galaxy, reveals the existence of a structured disk of ∼ 650 pc full diameter. The HCO distribution in the plane mimics the ring morphology displayed by other molecular/ionized gas tracers in M82. More precisely, rings traced by HCO, CO, and H II regions are nested, with the HCO ring lying in the outer edge of the molecular torus. Observations of HCO in Galactic clouds indicate that the abundance of HCO is strongly enhanced in the interfaces between the ionized and molecular gas. The surprisingly high overall abundance of HCO measured in M82 [$X(HCO) \sim 4 \times 10^{-10}$] indicates that its nuclear disk can be viewed as a giant photon-dominated region (PDR) of ≈ 650 pc size. The existence of various nested gas rings, with the highest HCO abundance occurring at the outer ring [$X(HCO) \sim 0.8 \times 10^{-9}$], suggests that PDR chemistry is propagating in the disk. We discuss the inferred large abundances of HCO in M82 in the context of a starburst evolutionary scenario, picturing the M82 nucleus as an evolved starburst.

Based on observations carried out with the Institut de Radioastronomie Millimétrique (IRAM) Plateau de Bure Interferometer. IRAM is supported by the Institut National des Sciences de l'Univers/Centre National de la Recherche Scientifique (France), the Max-Planck-Gesellschaft (Germany), and the Instituto Geográfico Nacional (Spain).

Appeared in: ApJ ***575****, L55*

ON THE HEATING SOURCE OF THE ORION KL HOT CORE

P.de Vicente(1), J.Martín-Pintado(1), R.Neri (2), A.Rodríguez-Franco
(1)Observatorio Astronómico Nacional, Campus Universitario, Apartado 1143, Alcalá de Henares, E-28800 Madrid, Spain, (2)Institut de Radioastronomie Millimétrique, 300 Rue de la Piscine, F-38406 Saint Martin d'Hères, France, (3)Escuela Universitaria de Optica, Departmento de Matemática Aplicada, Universidad Complutense de Madrid, Av. Arcos de Jalón s/n, 28037 Madrid, Spain

Abstract:

We present images of the J=10-9 rotational lines of HC3N in the vibrationally excited levels 1v7, 1v6, and 1v5 of the hot core (HC) in Orion KL. The images show that the spatial distribution and the size emission from the 1v7 and 1v5 levels are different. While the J=10-9 1v7 line has a size of $4'' \times 6''$ and peaks $1.1''$ northeast of the 3 mm continuum peak, the J=10-9 1v5 line emission is unresolved ($< 3''$) and peaks $1.3''$ south of the 3 mm peak. This is a clear indication that the HC is composed of condensations with very different temperatures (170 K for the 1v7 peak and > 230 K for the 1v5 peak). The temperature derived from the 1v7 and 1v5 lines increases with the projected distance to the suspected main heating source I. Projection effects along the line of sight could explain the temperature gradient as being produced by source I. However, the large luminosity required for source I ($> 5 \times 10^5 M_\odot$) to explain the 1v5 line suggests that external heating by this source may not dominate the heating of the HC. Simple model calculations of the vibrationally excited emission indicate that the HC can be internally heated by a source with a luminosity of $10^5 M_\odot$, located 1.2″southwest of the 1v5 line peak (1.8″south of source I). We also report the first detection of high-velocity gas from vibrationally excited HC3N emission.

Based on excitation arguments, we conclude that the main heating source is also driving the molecular outflow. We speculate that all the data presented in this Letter and the IR images are consistent with a young massive protostar embedded in an edge-on disk.

Appeared in: ApJ **574**, *L163*

MOLECULAR GAS AND DUST AT z = 2.6 IN SMM J14011+0252: A STRONGLY LENSED, ULTRALUMINOUS GALAXY, NOT A HUGE, MASSIVE DISK

D.Downes(1) and P.M.Solomon(2)
(1)Institute de Radio Astronomie Millimétrique, 300 rue de la Piscine, F-38406 St Martin d'Hères, France, (2)Astronomy Program, State University of New York, Stony Brook,NY 11794

Abstract:

We used the IRAM Interferometer to detect CO(3-2), CO(7-6), and 1.3 mm dust continuum emission from the submillimeter galaxy SMM J14011+0252 at a redshift of 2.6. Contrary to a recent claim that the CO was extended over 6.6″ (57 kpc), the new data yield a size of $2 \times 0.5''$ for the CO and the dust. Although previous results placed the CO peak in a region with no visible counterpart, the new maps show the CO and dust are centered on the J1 complex seen on K-band and optical images. We suggest the CO is gravitationally lensed not only by the foreground cluster A1835, but also by an individual galaxy on the line of sight. Comparison of measured and intrinsic CO brightness temperatures indicates the CO size is magnified by a factor of 25 ± 5.

After correcting for lensing, we derive a true CO diameter of $\approx 0.08''$ (700 pc), consistent with a compact circumnuclear disk of warm molecular gas similar to that in Arp 220. The high magnification means the true size, far-IR luminosity, star formation rate, CO luminosity, and molecular gas mass are all comparable with those in present-epoch ultraluminous IR galaxies, not with those of a huge, massive, early-universe galactic disk.

Accepted for publication in ApJ

THE OPACITY OF NEARBY GALAXIES FROM COUNTS OF BACKGROUND GALAXIES: II. LIMITS OF THE SYNTHETIC FIELD METHOD

R.A.González(1), L.Loinard(1), R.J. Allen(2) and S.Muller(3)
(1)Instituto de Astronomía, UNAM, Unidad Morelia, Michoacán, México, C.P. 58190, (2)Space Telescope Science Institute, Baltimore, MD 21218 (3)Institut de Radio Astronomie Millimétrique, F-38406 St. Martin d'Hères, France

Abstract:

Recently, we have developed and calibrated the Synthetic Field Method to derive the total extinction through disk galaxies. The method is based on the number counts and colors of distant background field galaxies that can be seen through the foreground object; it is the *only* method capable of determining extinction without *a priori* assumptions about the dust properties or its spatial distribution, and has been successfully applied to NGC 4536 and NGC 3664, two late–type galaxies located, respectively, at 16 and 11 Mpc.

Here, we study the applicability of the Synthetic Field Method to *HST* images of galaxies in the Local Group, and show that background galaxies cannot be easily identified through these nearby objects, even with the best resolution available today. In the case of M 31, each pixel in the *HST* images contains fifty to one hundred stars, and the background galaxies cannot be seen because of the intrinsic granularity due to strong surface brightness fluctuations. In the LMC, on the other hand, there is only about one star every six linear pixels, and the lack of detectable background galaxies results from a "secondary" granularity, introduced by structure in the wings of the point spread function.

The success of the Synthetic Field Method in NGC 4536 and NGC 3664 is a natural consequence of the reduction of the intensity of surface brightness fluctuations with distance. When the dominant confusion factor is structure in the PSF wings, as is the case of *HST* images of the LMC, and would be the case of M 31 images obtained with a 10-m diffraction-limited optical telescope, it becomes *in principle* possible to improve the detectability of background galaxies by subtracting the stars in the foreground object. However, a much better characterization of optical PSFs than is currently available would be required for an adequate subtraction of the wings. Given the importance of determining the dust content of Local Group galaxies, efforts should be made in that direction.

To appear in Astronomical Journal

THE LINE–OF–SIGHT DISTRIBUTION OF THE GAS IN THE INNER 60 PC OF THE GALAXY

B. Vollmer(1), R. Zylka(2,4) and W.J. Duschl(3,1)
(1)Max-Planck-Institut für Radioastronomie, Auf dem Hügel 69, 53121 Bonn, Germany, (2)Physikalisches Institut der Universität zu Köln, Zülpicher Str. 77, 50937 Köln, Germany, (3)Institut für Theoretische Astrophysik der Universität Heidelberg, Tiergartenstraße 15,69121 Heidelberg, Germany, (4)IRAM, 300 rue de la Piscine, 38406 St. Martin d'Hères, France

Abstract:

2MASS K_S band data of the inner 60 pc of the Galaxy

are used to reconstruct the line-of-sight distances of the giant molecular clouds located in this region. Using the 2MASS H band image of the same region two different populations of point sources are identified according to their flux ratio in the two bands. The population of blue point sources forms a homogeneous foreground that has to be subtracted before analyzing the K_S band image. The reconstruction is made using two basic assumptions: (i) an axis-symmetric stellar distribution in the region of interest and (ii) optical thick clouds with an area filling factor of ~1 that block all light of stars located behind them. Due to the reconstruction method the relative distance between the different cloud complexes is a robust result, whereas the absolute distance of structures located more than 10 pc in front of Sgr A* might be up to 30% larger than the one we derived from the data. It is shown that all structures observed at 1.2 mm continuum and in the CS(2-1) line are present in absorption. We place the 50 $\mathrm{km\,s^{-1}}$ cloud complex close to, but in front of Sgr A*. The 20 $\mathrm{km\,s^{-1}}$ cloud complex is located in front of the 50 $\mathrm{km\,s^{-1}}$ cloud complex and has a large LOS distance gradient along the direction of the galactic longitude. The Circumnuclear Disk is not seen in absorption. This leads to an upper limit of the cloud sizes within the Circumnuclear Disk of ~0.06 pc.

Accepted for publication in A&A

New Preprints

569. ABUNDANT MOLECULAR GAS IN THE INTERGALACTIC MEDIUM OF STEPHAN's QUINTET
U. Lisenfeld, J. Braine, P.-A. Duc, S. Leon, V. Charmandaris, E. Brinks
2002, *Astronomy and Astrophysics*

The IRAM Newsletter is edited by Michael Bremer at IRAM-Grenoble (e-mail address: `bremer@iram.fr`). In order to reduce costs we are now sending paper copies of this Newsletter to astronomical libraries only. The IRAM Newsletter is available in electronic form:

- by using the World Wide Web: from the IRAM home page (`http://iram.fr/`), click on item "Newsletter" and follow the links...
- by means of an anonymous `ftp` account, opened at IRAM for Internet users. To access those files, please connect through `ftp` to `iram.fr` (or `193.48.252.22`) and read the `README` file. Several subdirectories are available:

Directory	Contents
`/dist/newsletter`	Recent issues of this Newsletter (one subdirectory per issue)
e.g. `/dist/newsletter/jul95`	jul95.ps is the Postscript file for the July 1995 issue.
`/dist/doc`	Documentation on IRAM telescopes and software
`/dist/proposal`	Proposal forms and Latex files to aid proposal preparation
`/dist/soft`	distribution files for reduction software

- by means of an electronic mail file server installed at IRAM (on iraux2). This file server is a file distribution service that uses electronic mail facilities to deliver files. To communicate with it you should send a message to the electronic address:

  `listserv@iram.fr`

  On the first time you should send a message: `SUBSCRIBE IRAMNEWS` *your name*

  in order to subscribe to the mailing list IRAMNEWS. You will then receive an acknowledgement from the server. Then, for instance, to obtain a copy of the January 1999 issue, just send the one line message:

  `GET IRAMNEWS JAN99.PS`

  to the above electronic address. You will receive later a mail message containing the IRAM Newsletter in Postscript code. Please discard all the e-mail header information with a text editor, and send the file to a Postscript printer. More information may be obtained by sending the one line message:

  `HELP`

  Note that this file server also contains the proposal forms.

The e-mail list IRAMNEWS is used to send warning messages when the Newsletter is available, but also to provide fast information, if needed.

Please keep M. Bremer informed of any problem you may encounter.

IRAM Addresses:

	Address:	Telephone:	Fax:
Grenoble	Institut de Radioastronomie Millimétrique, 300 rue de la Piscine, Domaine Universitaire, 38406 St Martin d'Hères Cedex, France		
	from abroad:	(33) 476 82 49 00	(33) 476 51 59 38
	from France:	0 476 82 49 00	0 476 51 59 38
Plateau de Bure	Institut de Radioastronomie Millimétrique, Observatoire du Plateau de Bure, 05250 St Etienne en Dévoluy, France		
	from abroad:	(33) 492 52 53 60	(33) 492 52 53 61
	from France:	0 492 52 53 60	0 492 52 53 61
Granada	Instituto de Radioastronomía Milimétrica, Avenida Divina Pastora 7, Núcleo Central, 18012 Granada, España	(34) 958 80 54 54	(34) 958 22 23 63
Pico Veleta	Instituto de Radioastronomía Milimétrica, Estación Radioastronómica IRAM-IGN del Pico Veleta, Sierra Nevada, 18012 Granada, España	(34) 958 48 20 02	(34) 958 48 11 48

E-Mail Addresses:

- IRAM-Grenoble: `username@iram.fr`
- IRAM-Granada: `username@iram.es`

The `username` is generally the last name of the person to be contacted.